Chapter 6

Relic Abundance of Dark Matter with $\Delta(54)$ Flavor Symmetry

In this work we discuss the neutrino phenomenology in a $\Delta(54)$ discrete flavor symmetry and evaluate the relic abundance of dark matter (DM) and active neutrino-DM mixing angle considering various cosmological constraints. We introduced two Standard Model Higgs particles along with vector-like fermions and a new particle (S) which is a gauge singlet in the Standard Model. This modification leads to a mass matrix that diverges from the tribimaximal neutrino mixing pattern resulting in a non-zero reactor angle (θ_{13}). We also incorporated a $Z_2 \otimes Z_3 \otimes Z_4$ symmetry for the specific interactions in our model. The additional particle S is a sterile neutrino which is considered to be a probable dark matter candidate with mass in keV range.

6.1 Introduction

The observation of neutrino masses and their flavor mixing, as evidenced by neutrino oscillations, raises a question regarding the origin of their masses. [1–5]. It seems extremely unlikely that neutrino masses function in the same way as the masses of charged fermions as the standard model does not contain right-handed neutrinos, in contrast to other fermions. Several models outside of the standard

model (BSM) provide explanation for the the formation of neutrino masses, including the seesaw mechanism [6–8], radiative seesaw mechanism [9], extra-dimensional models [10, 11] and others. These references includes many current reviews on neutrino physics[12–29].

This work introduces a method based on the $\Delta(54)$ flavour symmetry framework with the inverse seesaw mechanism. Heterotic string models on factorizable orbifolds, such as the T^2/Z_3 orbifold, can exhibit the $\Delta(54)$ symmetry. Within these string models, doublets are not detected as basic modes but only singlets and triplets are detected. However, in magnetized/intersecting D-brane models, doublets may develop into basic modes. The nice feature of $\Delta(54)$ flavor symmetry is that there are also doublets that can be used for the quark sector. We can also suggest an extension to the Standard Model, utilizing $\Delta(54)$ symmetry. To represent quarks in different ways, we may work with the singlets $(1_1, 1_2)$ and doublets $(2_1, 2_2, 2_3, 2_4)$ representations of $\Delta(54)$. This extension essentially includes the latest experimental data on a number of quark sector features, including three quark mixing angles, six quark masses, and the CP-violating phase [30].

The neutrino phenomenology of the inverse see-saw is dependant upon the presence of an additional singlet fermion. According to this formalism, the lightest neutrino mass matrix is $M_\nu \approx M_d(M_T)^{-1}\mu M^{-1}{M_d}^T$, where M denotes the lepton number conserving interaction between right-handed and sterile fermions, and M_d is the Dirac mass term. Three more right-handed neutrinos and one gauge singlet chiral fermion field S as a sterile neutrino are added to the standard model particles in the Minimal Extended see-saw (MES), which is an extension of the canonical type-I see-saw. The 6×6 active-sterile neutrino mass matrix in this formalism is given by

$$M_\nu^{6\times 6} = -\begin{pmatrix} M_D M_R^{-1} M_D^T & M_D M_R^{-1} M_S^T \\ M_S (M_R^{-1})^T M_D^T & M_S M_R^{-1} M_S^T \end{pmatrix} \tag{6.1}$$

where M_D, M_R and M_S are the Dirac, Majorana and Sterile neutrino mass matrices. The Sterile neutrino mass is given as $m_s \simeq -M_S M_R^{-1} M_S^T$.

Neutrinos with sub-eV can be produced from M_D at the electroweak scale,

M_R at the TeV scale, and M_S at the keV scale. There are other important lines of evidence for dark matter (DM), such as Fritz Zwicky's 1933 observations of galaxy clusters, gravitational lensing (which Zwicky 1937 proposed could allow galaxy clusters to act as gravitational lenses), galaxy rotation curves in 1970, cosmic microwave background, and the most recent cosmology data provided by the Planck satellite. It is known that dark matter (DM) makes up around 27% of the universe, which is almost five times more than baryonic matter, based on the most current data from the Planck spacecraft. According to reports, the current dark matter abundance is given as[31]

$$\Omega_{DM}h^2 = 0.1187 \pm 0.0017$$

The physics community has faced enormous challenges in its search for potential dark matter candidates with new mechanisms beyond the standard model. The important criteria that a particle must have in order to be taken into consideration as a viable DM candidate. All of the SM particles are not eligible to be DM candidates due to these restrictions. The particle physics community became motivated to investigate several BSM frameworks that may provide accurate DM phenomenology and can be evaluated in many experiments.

The chapter is structured as follows: In sect 6.2, we introduce the $\Delta(54)$ discrete symmetry with inverse seesaw mechanism and discuss the characteristics of the flavor group relevant to constructing the model. In sect 6.3, we outline the allowable range for model parameters based on the constraints imposed by the 3σ range of neutrino oscillation data. In sect 6.4, we summarize the sterile dark matter and Ly-α constraints. In sect 6.5, we conclude our study and provide numerical results within the model.

6.2 Stucture of the Model

For the implementation of the Inverse Seesaw mechanism, the fermion sector must be extended within the Standard Model framework. We have introduced vector-like (VL) fermion denoted as N which have the property of being gauge singlets

inside the SM framework. We also introduced a gauge singlet denoted as S, which is considered to be a dark matter candidate in our model. In fact, the VEV of ϕ induces the mass term for the S fermion. We extended the model by a gauge singlet fermion. The main motivation of this extended field is to incorporate dark matter phenomenology in our model. The $\Delta(54)$ group includes irreducible representations 1_1, 1_2, 2_1, 2_2, 2_3, 2_4, $3_{1(1)}$, $3_{1(2)}$, $3_{2(1)}$ and $3_{2(2)}$.

Field	L	l	H	H'	N	S	χ	χ'	ζ	ξ	Φ_S	ϕ
$\Delta(54)$	$3_{1(1)}$	$3_{2(2)}$	1_1	1_2	$3_{1(1)}$	$3_{2(2)}$	1_2	2_1	1_2	$3_{2(1)}$	$3_{1(1)}$	$3_{1(2)}$
Z_2	1	-1	1	1	-1	1	-1	-1	-1	-1	-1	1
Z_3	ω	ω	1	1	1	1	1	1	1	ω	ω	1
Z_4	1	-1	1	1	1	1	-1	-1	1	1	1	1
U(1)	1	1	0	0	1	1	0	0	0	0	0	0

Table 6.1: Particle content of our model

We developed a model based on the $\Delta(54)$ disrete symmetry with inclusion of additional flavons namely χ, χ', ζ, ξ, Φ_S and ϕ. In order to avoid undesired interactions, we added additional symmetry $Z_2 \otimes Z_3 \otimes Z_4$. Details on the particle charge assignment and composition according to the flavor group are given in Table 6.1. The left-handed leptons doublets and the right-handed charged lepton are assigned using the triplet representation of $\Delta(54)$.

The Lagrangian is as follows :

$$\begin{aligned}\mathcal{L} =& \frac{y_1}{\Lambda}(l\bar{L})\chi H + \frac{y_2}{\Lambda}(l\bar{L})\chi' H + \frac{\bar{L}\tilde{H'}N}{\Lambda}y_\xi \xi + \frac{\bar{L}\tilde{H}N}{\Lambda}y_s\Phi_s + \frac{\bar{L}\tilde{H'}N}{\Lambda}y_a\Phi_s \\ &+ y_{NS}\bar{N^c}S\zeta + \frac{y_{s_1}}{\Lambda^2}\bar{S}S^c\phi \end{aligned} \tag{6.2}$$

The VEVs are naturally considered as,

$$\langle\chi\rangle = (v_\chi) \qquad \langle\chi'\rangle = (v_{\chi'}, v_{\chi'}) \quad \langle\Phi_S\rangle = (v_s, v_s, v_s) \quad \langle\xi\rangle = (v_\xi, v_\xi, v_\xi)$$
$$\langle\phi\rangle = (v_\phi, v_\phi, v_\phi) \quad \langle\zeta\rangle = (v_\zeta)$$

The charged lepton mass matrix is given as [32]

$$M_l = \frac{y_1 v}{\Lambda}\begin{pmatrix} v_\chi & 0 & 0 \\ 0 & v_\chi & 0 \\ 0 & 0 & v_\chi \end{pmatrix} + \frac{y_2 v}{\Lambda}\begin{pmatrix} -\omega v_{\chi'} + v_{\chi'} & 0 & 0 \\ 0 & -\omega^2 v_{\chi'} + \omega^2 v_{\chi'} & 0 \\ 0 & 0 & -v_{\chi'} + \omega v_{\chi'} \end{pmatrix}$$

where y_1 and y_2 are coupling constants.

6.2.1 Effective neutrino mass matrix

The Lagrangian may be used to construct the mass matrices related with the neutrino sector after applying $\Delta(54)$ and electroweak symmetry breaking. The M_S scale is an essential assumption of the ISS theory, providing small neutrino masses. To reduce the right-handed neutrino masses to the TeV scale, the M_S scale must be at the keV level. The inverse seesaw model is a TeV-scale seesaw model that permits heavy neutrinos remain as light as a TeV and Dirac masses to be as large as those of charged leptons, while maintaining compatibility with light neutrino masses in the sub-eV range.

$$M_{NS} = y_{NS}\begin{pmatrix} v_\zeta & 0 & 0 \\ 0 & v_\zeta & 0 \\ 0 & 0 & v_\zeta \end{pmatrix} \tag{6.3}$$

$$M_{\nu N} = \frac{v}{\Lambda}\begin{pmatrix} y_\xi v_\xi & y_s v_s + y_a v_a & y_s v_s - y_a v_a \\ y_s v_s - y_a v_a & y_\xi v_\xi & y_s v_s + y_a v_a \\ y_s v_s + y_a v_a & y_s v_s - y_a v_a & y_\xi v_\xi \end{pmatrix} \tag{6.4}$$

The Sterile neutrino mass matrix can be written as,

$$M_S = \frac{y_{s_1}}{\Lambda^2}\begin{pmatrix} v_\phi & 0 & 0 \\ 0 & v_\phi & 0 \\ 0 & 0 & v_\phi \end{pmatrix} \tag{6.5}$$

In the Inverse seesaw framework, the effective neutrino mass matrix can be written as

$$m_\nu = M_{\nu N} M_{NS}^{-1} M_S M_{NS}^{-1} M'_{\nu N} \tag{6.6}$$

The resultant mass matrix from Eq. (6.6)

$$m_\nu = v^2 \begin{pmatrix} \frac{s}{M^2}(2a^2+2c^2+x^2) & \frac{s}{M^2}(-a^2+c^2+2cx) & \frac{s}{M^2}(-a^2+c^2+2cx) \\ \frac{s}{M^2}(-a^2+c^2+2cx) & \frac{s}{M^2}(2a^2+2c^2+x^2) & \frac{s}{M^2}(-a^2+c^2+2cx) \\ \frac{s}{M^2}(-a^2+c^2+2cx) & \frac{s}{M^2}(-a^2+c^2+2cx) & \frac{s}{M^2}(2a^2+2c^2+x^2) \end{pmatrix} \tag{6.7}$$

where $a = \frac{y_a v_s v}{\Lambda}$, $c = \frac{y_s v_s v}{\Lambda}$, $x = \frac{y_\varepsilon v_\varepsilon v}{\Lambda}$, $s = \frac{y_{s_1} v_\phi}{\Lambda^2}$ and $M = y_{_{NS}} v_\zeta$. The dimension of the problem is absorbed by the term v and the components of the matrix are unaffected . Phase redefinitions of the charged lepton fields can absorb the phase of v, allowing it to be considered as a real parameter without losing generality [33].

The 6×6 active sterile neutrino mass matrix represented as in Eq.6.1 becomes,

$$M_\nu^{6\times 6} = \begin{pmatrix} \begin{pmatrix} -\frac{v^2(2a^2+2c^2+x^2)}{M\Lambda^2} & \frac{v^2(a^2-c^2+2cx)}{M\Lambda^2} & \frac{v^2(a^2-c^2+2cx)}{M\Lambda^2} \\ \frac{v^2(a^2-c^2+2cx)}{M\Lambda^2} & -\frac{v^2(2a^2+2c^2+x^2)}{M\Lambda^2} & \frac{a^2-c^2+2cx}{M\Lambda^2} \\ \frac{a^2-c^2+2cx}{M\Lambda^2} & \frac{a^2-c^2+2cx}{M\Lambda^2} & -\frac{v^2(2a^2+2c^2+x^2)}{M\Lambda^2} \end{pmatrix} & \begin{pmatrix} -\frac{svx}{M} & -\frac{(a+c)sv}{M\Lambda} & \frac{(a-c)sv}{M\Lambda} \\ \frac{(a-c)sv}{M\Lambda} & -\frac{svx}{M\Lambda} & -\frac{(a+c)sv}{M\Lambda} \\ -\frac{(a+c)sv}{M\Lambda} & \frac{(a-c)sv}{M\Lambda} & -\frac{svx}{M\Lambda} \end{pmatrix} \\ \begin{pmatrix} -\frac{svx}{M\Lambda} & \frac{(a-c)sv}{M\Lambda} & -\frac{(a+c)s}{M\Lambda} \\ -\frac{(a+c)s}{M\Lambda} & -\frac{svx}{M\Lambda} & -\frac{(a-c)sv}{M\Lambda} \\ \frac{(a-c)sv}{M\Lambda} & -\frac{(a+c)sv}{M\Lambda} & -\frac{svx}{M\Lambda} \end{pmatrix} & \begin{pmatrix} -\frac{s^2}{M} & 0 & \\ 0 & -\frac{s^2}{M} & 0 \\ 0 & 0 & -\frac{s^2}{M} \end{pmatrix} \end{pmatrix} \tag{6.8}$$

The final neutrino mixing matrix for the active-sterile mixing takes the form as,

$$V \simeq \begin{pmatrix} (1-\frac{1}{2}RR^\dagger)U & R \\ -R^\dagger U & 1-\frac{1}{2}RR^\dagger \end{pmatrix} \tag{6.9}$$

where $R = M_D M_R^{-1} M_S^T (M_S M_R^{-1} M_S^T)$ is a 3×3 matrix representing the strength of active sterile mixing and U is the leptonic mass matrix for active neutrinos [34].

$$R \simeq \begin{pmatrix} \frac{s^3 vx}{M^2\Lambda} & \frac{s^3 v(a+c)}{M^2\Lambda} & \frac{s^3 v(-a+c)}{M^2\Lambda} \\ \frac{s^3 v(-a+c)}{M^2\Lambda} & \frac{s^3 vx}{M^2\Lambda} & \frac{s^3 v(a+c)}{M^2\Lambda} \\ \frac{s^3 v(a+c)}{M^2\Lambda} & \frac{s^3 v(-a+c)}{M^2\Lambda} & \frac{s^3 vx}{M^2\Lambda} \end{pmatrix} \tag{6.10}$$

The neutrino mass matrix m_ν can be diagonalized by the PMNS matrix U as

$$U^\dagger m_\nu^{(i)} U^* = \mathrm{diag}(m_1, m_2, m_3) \tag{6.11}$$

We can analytically calculate U using the relation $U^\dagger h U = \mathrm{diag}(m_1^2, m_2^2, m_3^2)$, where $h = m_\nu m_\nu^\dagger$. We followed the framework of Adhikary et al. [35] for calculating oscillation parameters of a generalized neutrino mass matrix. The row-wise elements of U are given in terms of the elements of the h and its eigenvalues m_i^2.

$$U_{1i} = \frac{(h_{22} - m_i^2)h_{13} - h_{12}h_{23}}{N_i} \tag{6.12}$$

$$U_{2i} = \frac{(h_{11} - m_i^2)h_{23} - h_{12}^* h_{13}}{N_i} \tag{6.13}$$

$$U_{3i} = \frac{|h_{12}|^2 - (h_{11} - m_i^2)(h_{22} - m_i^2)}{N_i} \tag{6.14}$$

6.3 Numerical Analysis

The mass matrix in Eq. (6.7) gives the effective neutrino mass matrix in terms of the model complex parameters a, c, and x. We can find the parameter values of the model by fitting the model to the current neutrino oscillation data. We use the 3σ interval for the neutrino oscillation parameters ($\theta_{12}, \theta_{23}, \theta_{13}, \Delta m_{21}^2, \Delta m_{31}^2$) as presented in Table 6.2. One may refer to Esteban, I. et al., NuFIT-6.0 for the latest NuFIT data 2024 [36]. A constraint was applied on the sum of absolute neutrino masses from the cosmological bound $\sum_i m_i < 0.12eV$. In our study, the three complex parameters of the model are treated as free parameters and are allowed to run over the following ranges: $|a| \in [0, 1]eV$, $\phi_a \in [-\pi, \pi]$, $|c| \in [0, 10^{-1}]eV$,

$\phi_c \in [-\pi, \pi]$, $|x| \in [0, 10^{-3}]eV$, $\phi_x \in [-\pi, \pi]$. The two real parameters are allowed to run over the ranges: $M \in [10^{13}, 10^{14}]eV$, $s \in [10^8, 10^9]eV$
where ϕ_a , ϕ_c and ϕ_x are the phases.

Parameters	NH (3σ)	IH (3σ)
$\Delta m^2_{21}[10^{-5}eV^2]$	$6.92 \to 8.05$	$6.92 \to 8.05$
$\Delta m^2_{31}[10^{-3}eV^2]$	$2.463 \to 2.606$	$-2.584 \to -2.438$
$\sin^2\theta_{12}$	$0.275 \to 0.345$	$0.275 \to 0.345$
$\sin^2\theta_{13}$	$0.02023 \to 0.02376$	$0.02053 \to 0.02397$
$\sin^2\theta_{23}$	$0.430 \to 0.596$	$0.437 \to 0.597$
δ_{CP}	$96^\circ \to 422^\circ$	$201^\circ \to 348^\circ$

Table 6.2: The neutrino oscillation parameters from NuFIT 6.0 (2024) [36]

The neutrino mass matrix m_ν can be diagonalized by the PMNS matrix U as follow [33]:

$$U^\dagger m_\nu U^* = \text{diag}(m_1, m_2, m_3) \tag{6.15}$$

We numerically calculated U using the relation $U^\dagger h U = \text{diag}(m_1^2, m_2^2, m_3^2)$, where $h = m_\nu m_\nu^\dagger$. The neutrino oscillation parameters θ_{12}, θ_{13}, θ_{23} and δ can be obtained from U as

$$s_{12}^2 = \frac{|U_{12}|^2}{1 - |U_{13}|^2}, \qquad s_{13}^2 = |U_{13}|^2, \qquad s_{23}^2 = \frac{|U_{23}|^2}{1 - |U_{13}|^2} \tag{6.16}$$

and δ may be given by

$$\delta = \sin^{-1}\left(\frac{8\,\text{Im}(h_{12}h_{23}h_{31})}{P}\right) \tag{6.17}$$

with

$$P = (m_3^2 - m_2^2)(m_2^2 - m_1^2)(m_3^2 - m_1^2)\sin 2\theta_{12}\sin 2\theta_{23}\sin 2\theta_{13}\cos\theta_{13} \tag{6.18}$$

We measured the difference between the neutrino mixing parameters and the latest experimental data by minimizing the resulting χ^2 function, which allowed

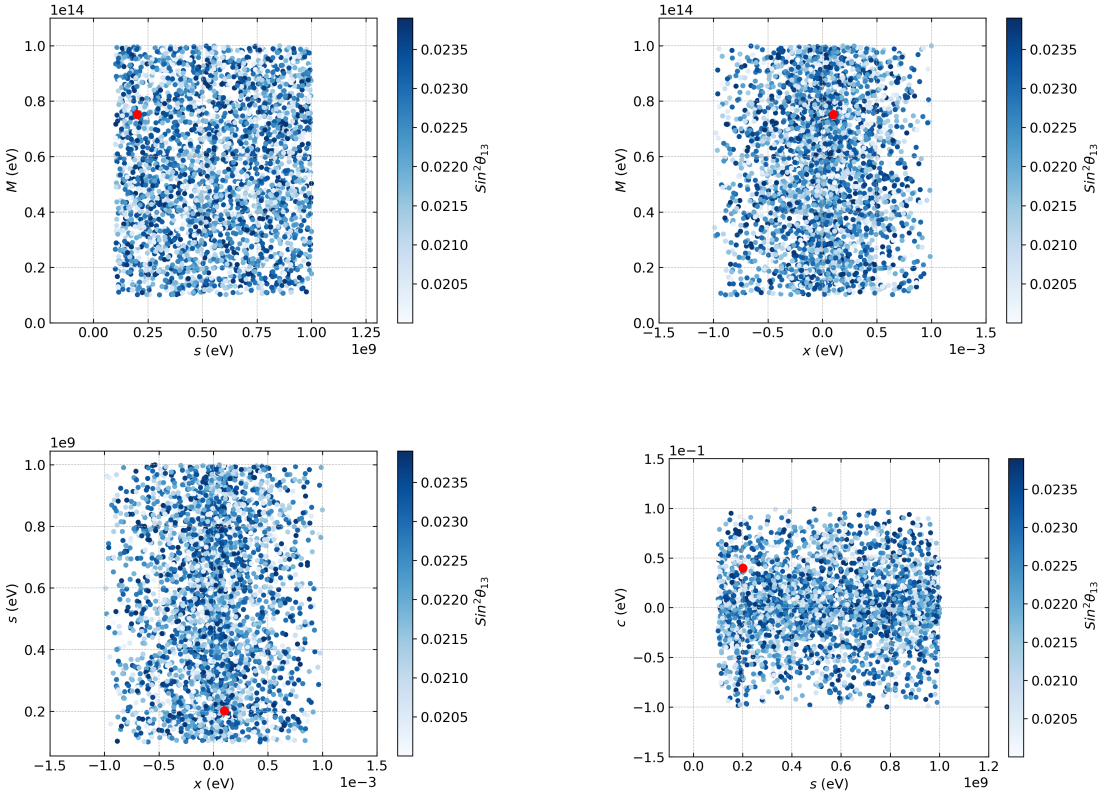

Figure 6.1: Correlation between the parameters x, s, a, M and s . The red dot marker indicates the best-fit values corresponding to χ^2 min.

us to modify the $\Delta(54)$ model to fit the experimental data:

$$\chi^2 = \sum_i \left(\frac{\lambda_i^{model} - \lambda_i^{expt}}{\Delta\lambda_i} \right)^2 , \tag{6.19}$$

where λ_i^{model} is the i^{th} observable predicted by the model, λ_i^{expt} stands for i^{th} experimental best-fit value and $\Delta\lambda_i$ is the 1σ range of the observable.

The best-fit values for x, c and a obtained are 0.109×10^{-3} eV, 0.401×10^{-1} eV and 0.105×10^{-1} eV respectively. The values of M and s are 0.752×10^{14} eV and 0.201×10^{9} eV respectively. These values are used further to calculate the neutrino oscillation parameters of our model.

Correspondingly, the best-fit values for the neutrino oscillation parameters are, $\sin^2\theta_{12} = 0.31940$, $\sin^2\theta_{13} = 0.02394$, $\sin^2\theta_{23} = 0.51231$, $\sin\delta_{CP} = 0.094$. The best-fit values for other parameters, such as $\Delta m^2_{21}/\Delta m^2_{31}$ is 0.029, which corresponds to the χ^2-minimum.

The Sterile mass is obtained as [34]:

$$m_s = \frac{s^2}{M} \tag{6.20}$$

which is considered as the dark matter mass and is represented as M_{DM} in our analysis.

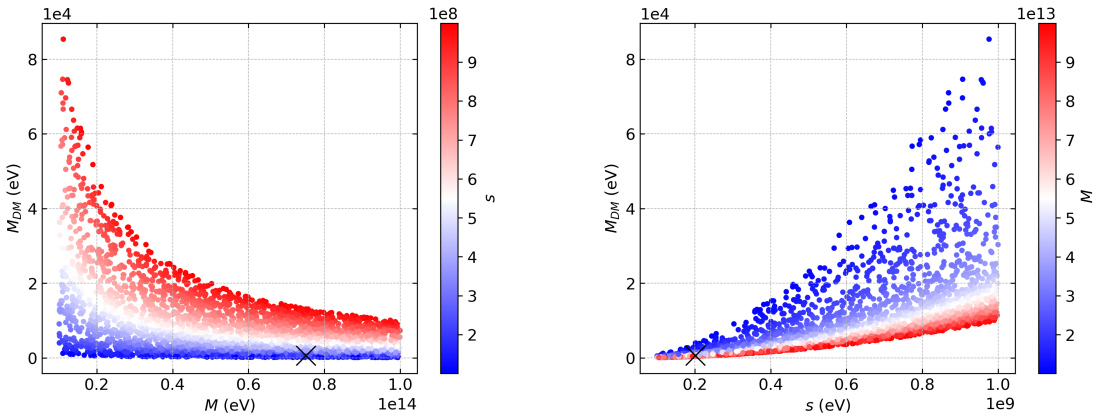

Figure 6.2: Allowed regions of the parameter M_{DM} . The best fit values are indicated by cross marker.

6.4 Sterile Dark Matter

A non-resonantly created sterile dark matter (DM) may be easily accommodated within an extended SM of particle physics. Since the mass of the sterile neutrino is limited to a few keV, it is a strong candidate for warm dark matter. The only way the sterile neutrinos interact with the particles of the standard model is via mixing with the active neutrinos. Thus, the DM abundance can ultimately build up from the active neutrinos that are a part of the original plasma (because they interact weakly). This mechanism is known as the Dodelson and Widrow (DW) mechanism [37, 38].

When lepton asymmetry is absent, sterile neutrino non-resonant production (NRP) occurs. On the other hand, resonant sterile neutrinos with tiny mixing angles can be produced for a convincing amount of lepton asymmetry in the original

plasma, leading to noticeably cooler momenta. Another name for this process is the resonant production mechanism, or Shi and Fuller (SF) [39]. Non-resonant production accounts for the smallest amount of dark matter contribution that can be created as a result of the dark matter mass and the mixing angle. As a non-resonant DM candidate, we have taken into account a singlet fermion (S) in our model. Therefore m_{DM} will be used to represent the fermion mass.

We solve the parameters of the model with some fixed values of variables such as the M in the range $10^{13} - 10^{14}$ GeV. Additionally, the gauge singlet S is considered with a mass between 10^8 and 10^9 eV. By calculating these values, we are able to obtain the mixing angle $sin^2(2\theta_{DM})$ that satisfies the cosmological constraints as well as the required mass m_{DM} in the keV range. In our study, the non-vanishing components V_{14} and V_{34} of the mixing matrix V, contribute to the mixing angles. For any species, the relic abundance may be expressed as [40],

$$\Omega h^2 = \frac{\rho_{x_o}}{\rho_{crit}} = \frac{s_o Y_\infty m}{\rho_{crit}} \tag{6.21}$$

where, ρ_{crit} is the critical energy density of the universe, ρ_{x_o} is present energy density of x, Y_∞ is the present abundance of the particle x and s_o is the present day entropy. Also we can get the values of $\rho_{crit} \approx 1.054 \times 10^{-5}$ h^2 GeV cm^{-3} and $s_o \approx 2886$ cm^{-3} from Particle Data Group (PDG). For sterile neutrinos, it can be expressed as[41]:

$$\Omega_{\alpha x} = \frac{m_x Y_{\alpha x}}{3.65 \times 10^{-9} \mathrm{h^2 GeV}} \tag{6.22}$$

where $\alpha = e, \mu, \tau$. According to the active-sterile mixing and the sterile mass, which is proportional to the resultant relic abundance of a sterile neutrino state with a non-vanishing mixing to the active neutrinos is expressed as [42, 43],

$$\Omega_{\alpha S} h^2 = 1.1 \times 10^7 \sum C_\alpha(m_s) |V_{\alpha s}|^2 (\frac{m_s}{\mathrm{keV}})^2 \tag{6.23}$$

where,

$$C_\alpha = 2.49 \times 10^{-5} \frac{Y_{\alpha s} \mathrm{keV}}{sin^2(\theta_{\alpha s}) m_s} \tag{6.24}$$

Using the solution of the Boltzmann equation [44], C_α, the active flavor-dependent coefficients, may be determined numerically. We replace s with DM in the following formula for relic abundance, taking into account the sterile neutrino as a

potential dark matter candidate and using the parametrization $|V_{\alpha s} \simeq sin(\theta_{\alpha s})|$. Consequently, the relic abundance simplified equation for non-resonantly generated dark matter takes the form [41, 45]:

$$\Omega_{DM}h^2 \simeq 0.3 \times 10^{10} Sin^2(2\theta_{DM})(\frac{M_{DM} \times 10^{-2}}{\text{keV}})^2 \tag{6.25}$$

where, Ω_{DM} is directly proportional to m_{DM} which is the DM mass as mentioned earlier and $sin^2(2\theta_{DM})$ viz the active-DM mixing angle with $sin^2(2\theta_{DM}) = 4(V_{14}^2 + V_{34}^2)$. Here, V_{14}^2 and V_{34}^2 are the 14 and 34 element of the V matrix in Eq.6.9.

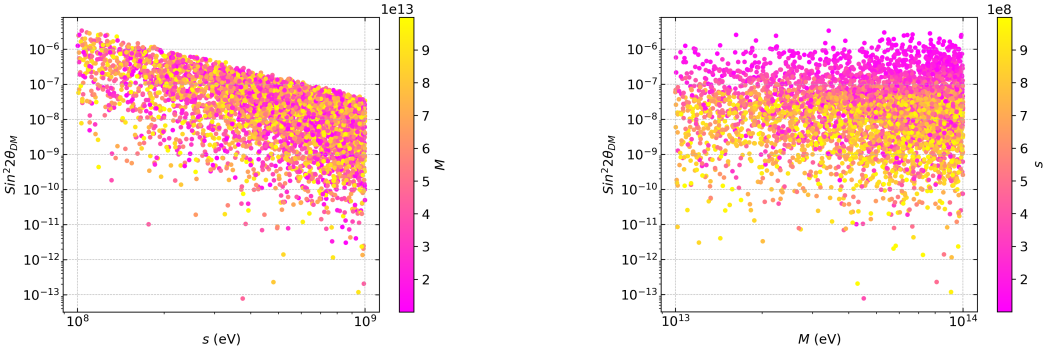

Figure 6.3: Allowed regions of Active neutrino-DM mixing angle ($Sin^2\theta_{DM}$) as a function of Gauge singlet mass (s) and RHN mass (M) respectively.

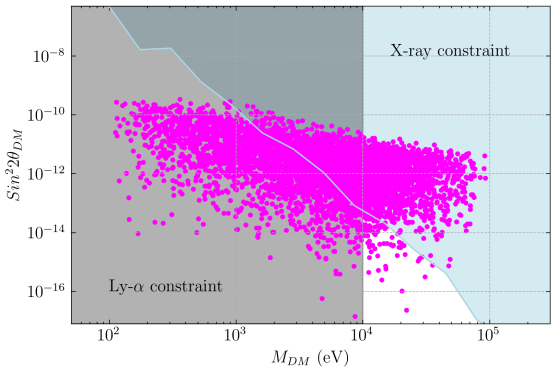

Figure 6.4: Correlation between Active neutrino-DM mixing angle ($Sin^2\theta_{DM}$) as a function of dark matter mass (M_{DM}) including constraints from Lyman-α and X-ray for NH.

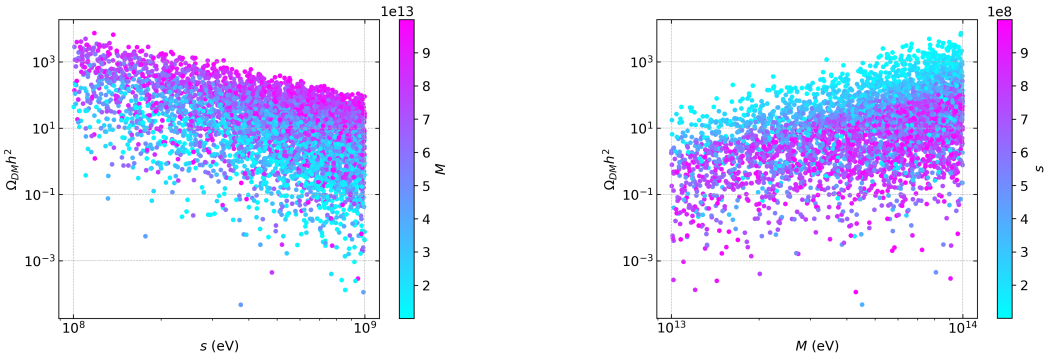

Figure 6.5: Allowed regions of Relic abundance ($\Omega_{DM}h^2$) as a function of Gauge singlet mass (s) and RHN mass (M) respectively.

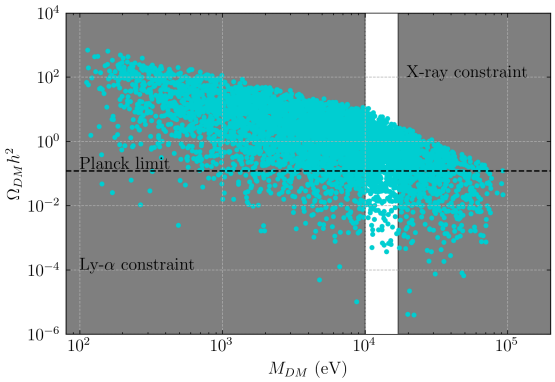

Figure 6.6: Correlation between Relic abundance ($\Omega_{DM}h^2$) as a function of dark matter mass (M_{DM}) and including constraints from Lyman-α and X-ray for NH.

6.5 Conclusion

We demonstrated the $\Delta(54)$ flavor symmetry along with the $Z_2 \otimes Z_3 \otimes Z_4$ symmetry which results in neutrino mass matrices and the subsequent predictions are consistent with the neutrino experimental data and the cosmological constraints on the relic abundance of dark matter (DM) and active neutrino-DM mixing angle. The ISS mechanism is incorporated into our model to offer a flavor-symmetric approach. This involves the prediction of the CP violation, solar mixing angle, upper octant of atmospheric mixing angle, and non-zero reactor angle. The model best data agreement is found in the normal hierarchy case with minimum χ^2 analysis.

However, the inverted hierarchy scenario does not predict the model data with experimental findings. We calculated the sterile neutrino mass which is a potential dark matter (DM) candidate and the active neutrino-DM mixing angle with the predicted model parameters. The non-resonant formation of sterile neutrinos and the corresponding limitations from Lyman-α have been taken into consideration in this study. The active neutrino-DM mixing angle is examined in relation to DM mass. It is found that the data points from our model prefers the Lyman-α range in the case of NH. The constraints for Ly-α is 10 keV. The lower bound for X-ray constraint is approximately 17 keV [44]. We have shown a co-relation between dark matter mass and active-DM mixing angle. A very small region between 10 - 16 keV falls in the allowed parameter space for NH. We have shown the dark matter mass range which obeys the Planck limit for relic abundance of dark matter. We have larger number of points for in the allowed parameter space m_{DM} = 10 - 16 keV satisfying the Planck bound.Future dark matter and neutrino oscillation experiments such as DUNE, JUNO, Daya Bay and Super-Kamiokande may test the model considering the predictions of the model align with the most recent neutrino data.

Bibliography

[1] Aker, M. *et al.* Improved upper limit on the neutrino mass from a direct kinematic method by KATRIN. *Physical review letters* **123** (22), 221802, 2019.

[2] Faessler, A. Status of the determination of the electron-neutrino mass. *Progress in Particle and Nuclear Physics* 103789, 2020.

[3] Araki, T. *et al.* Measurement of neutrino oscillation with KamLAND: Evidence of spectral distortion. *Physical Review Letters* **94** (8), 081801, 2005.

[4] Cao, S. *et al.* Physics potential of the combined sensitivity of T2K-II, NOνA extension, and JUNO. *Physical Review D* **103** (11), 112010, 2021.

[5] Nath, A. & Francis, N. K. Detection techniques and investigation of different

neutrino experiments. *International Journal of Modern Physics A* **36** (13), 2130008, 2021.

[6] Minkowski, P. $\mu \to e\gamma$ at a rate of one out of 10^9 muon decays?. *Physics Letters B* **67** (4), 421–428, 1977.

[7] King, S. & Yanagida, T. Testing the see-saw mechanism at collider energies. *Progress of theoretical physics* **114** (5), 1035–1043, 2005.

[8] Mohapatra, R. N. Mechanism for understanding small neutrino mass in superstring theories. *Physical Review Letters* **56** (6), 561, 1986.

[9] Ma, E. Radiative inverse seesaw mechanism for nonzero neutrino mass. *Physical Review D* **80** (1), 013013, 2009.

[10] Mohapatra, R. N. *et al.* Neutrino masses and oscillations in models with large extra dimensions. *Physics Letters B* **466** (2-4), 115–121, 1999.

[11] Arkani-Hamed, N. *et al.* Neutrino masses from large extra dimensions. *Physical Review D* **65** (2), 024032, 2001.

[12] Nguyen, T. P. *et al.* Decay of standard model-like Higgs boson $h \to \mu\tau$ in a 3-3-1 model with inverse seesaw neutrino masses. *Phys. Rev. D* **97** (7), 073003, 2018. 1802.00429.

[13] King, S. F. *et al.* Neutrino Mass and Mixing: from Theory to Experiment. *New J. Phys.* **16**, 045018, 2014. 1402.4271.

[14] King, S. F. Neutrino mass models. *Rept. Prog. Phys.* **67**, 107–158, 2004. hep-ph/0310204.

[15] Cao, S. *et al.* Physics potential of the combined sensitivity of T2K-II, NOνA extension, and JUNO. *Phys. Rev. D* **103** (11), 112010, 2021. 2009.08585.

[16] Ahn, Y. H. & Gondolo, P. Towards a realistic model of quarks and leptons, leptonic CP violation, and neutrinoless $\beta\beta$-decay. *Phys. Rev. D* **91**, 013007, 2015. 1402.0150.

[17] McDonald, A. B. Nobel lecture: the sudbury neutrino observatory: observation of flavor change for solar neutrinos. *Reviews of Modern Physics* **88** (3), 030502, 2016.

[18] Nguyen, T. P. *et al.* Low-energy phenomena of the lepton sector in an A4 symmetry model with heavy inverse seesaw neutrinos. *PTEP* **2022** (2), 023B01, 2022. 2011.12181.

[19] Hong, T. T. *et al.* Decays $h \to e_a e_b$, $e_b \to e_a \gamma$, and $(g-2)_{e,\mu}$ in a $3-3-1$ model with inverse seesaw neutrinos. *PTEP* **2022** (9), 093B05, 2022. 2206.08028.

[20] Kajita, T. Nobel lecture: Discovery of atmospheric neutrino oscillations. *Reviews of Modern Physics* **88** (3), 030501, 2016.

[21] de Salas, P. F. *et al.* 2020 global reassessment of the neutrino oscillation picture. *Journal of High Energy Physics* **2021** (2), 1–36, 2021.

[22] Okada, H. & Tanimoto, M. Spontaneous CP violation by modulus τ in A4 model of lepton flavors. *Journal of High Energy Physics* **2021** (3), 1–27, 2021.

[23] Ahn, Y. H. *et al.* Toward a model of quarks and leptons. *Phys. Rev. D* **106** (7), 075029, 2022. 2112.13392.

[24] Phong Nguyen, T. *et al.* CP violations in a predictive A_4 symmetry model. *PTEP* **2020** (3), 033B04, 2020. 1711.05588.

[25] Buravov, L. I. Confining potential and mass of elementary particles. *J. Mod. Phys.* **7** (1), 129–133, 2017. 1502.00958.

[26] Buravov, L. Elementary muon, pion, and kaon particles as resonators for neutrino quanta. Calculations of mass ratios for e, μ, π^0, $\pi^\pm$, K^0, $K^\pm$, and ν_e. *Russian Physics Journal* **52**, 25–32, 2009.

[27] Barman, A. *et al.* Neutrino mixing phenomenology: A4 discrete flavor symmetry with type-I seesaw mechanism. *Modern Physics Letters A* **39** (07), 2350200, 2024.

[28] Bora, H. *et al.* Majorana neutrinos in Double Inverse Seesaw and $\Delta(54)$ Flavor Models. *International Journal of Modern Physics A* , 2024.

[29] Bora, H. *et al.* Neutrino mass model in the context of $\Delta(54) \otimes Z_2 \otimes Z_3 \otimes Z_4$ flavor symmetries with Inverse Seesaw mechanism. *Physics Letters B* **848**, 2023.

[30] Vien, V. An extension of the standard model with symmetry for quark masses and mixings. *Physics of Atomic Nuclei* **84** (2), 179–183, 2021.

[31] Taoso, M. *et al.* Dark matter candidates: a ten-point test. *Journal of Cosmology and Astroparticle Physics* **2008** (03), 022, 2008.

[32] Ishimori, H. *et al.* Lepton flavor model from $\Delta(54)$ symmetry. *Journal of High Energy Physics* **2009** (04), 011, 2009.

[33] Lei, M. & Wells, J. D. Minimally modified A_4 Altarelli-Feruglio model for neutrino masses and mixings and its experimental consequences. *Physical Review D* **102** (1), 016023, 2020.

[34] Zhang, H. Light sterile neutrino in the minimal extended seesaw. *Physics Letters B* **714** (2-5), 262–266, 2012.

[35] Adhikary, B. *et al.* Masses, mixing angles and phases of general majorana neutrino mass matrix. *Journal of High Energy Physics* **2013** (10), 1–25, 2013.

[36] Esteban, I. *et al.* Nufit-6.0: Updated global analysis of three-flavor neutrino oscillations. *arXiv preprint arXiv:2410.05380* , 2024.

[37] Kang, S. K. The sterile neutrino as dark matter. *NEW PHYSICS* **66** (8), 984–992, 2016.

[38] Palazzo, A. *et al.* Sterile neutrinos as subdominant warm dark matter. *Physical Review D—Particles, Fields, Gravitation, and Cosmology* **76** (10), 103511, 2007.

[39] Shi, X. & Fuller, G. M. New dark matter candidate: Nonthermal sterile neutrinos. *Physical Review Letters* **82** (14), 2832, 1999.

[40] Kolb, E. & Turner, M. The early universe, vol. 69 of frontiers in physics series, 1990.

[41] Asaka, T. *et al.* Lightest sterile neutrino abundance within the νmsm. *Journal of High Energy Physics* **2007** (01), 091, 2007.

[42] Abada, A. *et al.* Dark matter in the minimal inverse seesaw mechanism. *Journal of Cosmology and Astroparticle Physics* **2014** (10), 001, 2014.

[43] Ng, K. C. *et al.* New constraints on sterile neutrino dark matter from nustar m31 observations. *Physical Review D* **99** (8), 083005, 2019.

[44] Gautam, N. & Das, M. K. Phenomenology of kev scale sterile neutrino dark matter with s4 flavor symmetry. *Journal of High Energy Physics* **2020** (1), 1–34, 2020.

[45] Abazajian, K. *et al.* Sterile neutrino hot, warm, and cold dark matter. *Physical Review D* **64** (2), 023501, 2001.